https://doi.org/10.1038/s44298-025-00117-w

Borna disease virus 2 maintains genomic polymorphisms by superinfection in persistently infected cells

Takehiro Kanda[1,2], Pauline Dianne Santos[3], Dirk Höper[3], Martin Beer[3], Dennis Rubbenstroth[3] ✉ & Keizo Tomonaga[1,2,4] ✉

Mammalian orthobornaviruses, such as Borna disease virus 1 (BoDV-1) and variegated squirrel bornavirus 1, are zoonotic pathogens that cause fatal encephalitis in humans. BoDV-2, another mammalian orthobornavirus with high genetic homology to BoDV-1, is believed to share the same geographical distribution as BoDV-1, indicating its potential risk to human health. However, due to the limited number of isolations, the virological characteristics of BoDV-2, such as pathogenicity and infectivity, remain largely unexplored. Here, we re-evaluated the whole-genome sequence of BoDV-2 and established a reverse genetics system to investigate its virological properties. Compared to the published reference sequence, we identified two nonsynonymous nucleotide substitutions in the large (L) gene, one of which was critical for restoring polymerase activity, enabling the successful recovery of recombinant BoDV-2 (rBoDV-2). Additionally, we identified two nonsynonymous single-nucleotide polymorphisms (SNPs) in the L gene and one in the phosphoprotein (P) gene. Substitution of these SNPs significantly enhanced the growth ability of rBoDV-2. Furthermore, our studies demonstrated that BoDV-2 does not induce superinfection exclusion in cells, allowing the persistence of low-fitness genome variants for an extended period of time. These findings help to characterize the virological properties of BoDV-2 and shed light on how bornaviruses maintain genetic diversity in infected cells.

Viruses of the genus *Orthobornavirus* within the family *Bornaviridae* have been documented to infect a wide range of vertebrate species, including mammals and avians[1–3]. Currently, the genus comprises 25 viruses belonging to 9 different viral species[4]. Among these, *Orthobornavirus bornaense* consists of two mammalian viruses: Borna disease virus 1 (BoDV-1), the prototype of the family *Bornaviridae*, and BoDV-2, a genetically closely related virus to BoDV-1. BoDV-1 has been identified as the etiological agent of Borna disease (BD), a nonpurulent encephalomyelitis affecting horses, sheep, and other mammalian species[1,2]. Conversely, BoDV-2 was only isolated from a single case of a pony showing severe and incurable neurological symptoms in eastern Austria in 1999, where BoDV-1 was not endemic[5]. Although the genome sequence of BoDV-2 isolate No/98 shares approximately 80% nucleotide identity with that of BoDV-1 strains[6], its virological properties, including host range, replication ability, and pathogenicity, have not been fully elucidated.

The pathogenicity of BoDV-1 in humans was controversial until two case studies were reported in 2018; these studies demonstrated the presence of the BoDV-1 antigen and RNA in a healthy young man and in two organ transplant recipients who died of encephalitis[7,8]. Subsequently, several studies have reported that infection with BoDV-1 was associated with more than forty fatal cases of encephalitis in humans[9–15]. Additionally, variegated squirrel bornavirus 1 (VSBV-1; species *Orthobornavirus sciuri*) was isolated from squirrel breeders who died of encephalitis[16]. Therefore, both BoDV-1 and VSBV-1 are zoonotic pathogens that cause fatal encephalitis in humans[17]. However, the potential of BoDV-2 to infect and cause disease in humans remains unclear. Considering that BoDV-2 isolate No/98 was isolated from a pony that displayed fatal neurological disorders and that BoDV-2 is genetically more closely related to BoDV-1 than VSBV-1, it is likely that BoDV-2 may also possess zoonotic potential.

The reverse genetics system is a powerful tool for elucidating viral characteristics such as replication and pathogenesis. The reverse genetics of

[1]Laboratory of RNA Viruses, Department of Virus Research, Institute for Life and Medical Science, Kyoto University, Kyoto, Japan. [2]Department of Molecular Virology, Graduate School of Medicine, Kyoto University, Kyoto, Japan. [3]Institute of Diagnostic Virology, Friedrich-Loeffler-Institute, Greifswald, Germany. [4]Department of Mammalian Regulatory Network, Graduate School of Biostudies, Kyoto University, Kyoto, Japan. ✉e-mail: Dennis.Rubbenstroth@fli.de; tomonaga.keizo.5r@kyoto-u.ac.jp

BoDV-1 was initially described by Schneider et al. in 2005; a plasmid expressing the full-length BoDV-1 antigenome and three helper plasmids expressing the nucleoprotein (N), phosphoprotein (P), and large protein (L) encoding the RNA-dependent RNA polymerase were transfected into cells expressing T7 polymerase[18]. This system has been further improved by employing highly transfectable HEK293T cells for plasmid transfection and incorporating two helper plasmids expressing matrix protein (M) and glycoprotein (G)[19–21]. Given that the genomic components of BoDV-2 closely resemble those of BoDV-1, it is predicted that recombinant BoDV-2 (rBoDV-2) can be easily rescued by employing the same strategy as used for BoDV-1. However, although the complete genome sequence of BoDV-2 has been deposited in NCBI GenBank, previous studies have raised concerns about potential errors in the L gene, indicating the need to reassess the genome sequence of BoDV-2[6].

In this study, we aimed to investigate the virological properties of BoDV-2 using recombinant viral techniques and therefore redetermine the genome sequence of BoDV-2 isolate No/98, which has been maintained in persistently infected cells. We found two nonsynonymous nucleotide substitutions in the L gene compared to the published sequence. One of these substitutions was crucial for restoring the polymerase activity of L, allowing successful recovery of rBoDV-2 through reverse genetics. Additionally, we identified two nonsynonymous single-nucleotide polymorphisms (SNPs) in the L gene and one in the P gene. Substituting these SNPs significantly enhanced the growth ability of rBoDV-2. Furthermore, our study demonstrated that BoDV-2 does not induce superinfection exclusion in cells, leading to long-term maintenance of low-fitness genome variants in persistently infected cells.

Results

Reassessment of the complete genome sequence of BoDV-2

The complete genome sequence of BoDV-2 isolate No/98 is deposited in NCBI GenBank; however, it is suspected that this sequence might contain several errors in the L gene[6]. Therefore, we reassessed the whole-genome sequence of BoDV-2 isolate No/98 via a shotgun sequencing of total RNA extracted from persistently infected Vero cells available at the Friedrich-Loeffler-Institut. Compared to the published sequence (accession no. AJ311524), the reassessed sequence contains one and five nucleotide differences in the P and L genes, respectively (Fig. 1A). Two of them in the L gene, uracil at positions 2762 and 3334, which are located in the polyribonucleotidyltransferase (PRNTase) domain (Fig. 1B), were completely substituted with guanine, resulting in amino acid changes of leucine at position 921 with arginine and cysteine at position 1112 with glycine (Fig. 1A). In addition, three SNPs were detected in the L gene, two of which, positions 3743 and 4250, induce nonsynonymous amino acid changes in the C-terminal domain (CTD) of L (Fig. 1A and B). A nonsynonymous SNP was also detected at position 456 of the P gene (Fig. 1A). Furthermore, we performed rapid amplification of cDNA ends (RACE) analysis to determine the exact 3' and 5' terminal sequences. Similar to BoDV-1[18,22], BoDV-2 possesses four nucleotides overhung at the 3' end of both the genome and antigenome without a complementary sequence at the 5' end of the opposite strand (Fig. 1C). Compared to the published sequence, the reassessed sequence lacks uracil at the 5' end of the genome (Fig. 1D).

The polymerase activity of BoDV-2 L is restored by substituting a nucleotide

In the reassessed sequence, nucleotides at positions 2762 and 3334 of the L gene are completely substituted compared to the reference sequence (Fig. 1A). To determine whether these differences affect BoDV-2 L gene expression, we constructed L cDNA expression plasmids possessing each nucleotide substitution independently (BoDV-2 L_R or L_G) or in combination (BoDV-2 L_{RG}) and performed western blotting (Fig.2A). In a previous study, we could not detect expression of FLAG-tagged BoDV-2 L with the reference sequence, though that of FLAG-tagged BoDV-1 L was clearly demonstrated, suggesting the low expression potential of the FLAG-BoDV2 L construct[23]. However, in the present study, we could detect the expression of BoDV-2 L with the reference sequence when a linker sequence (N_{term}-GSSGGGGSGGGGSSG) was inserted between FLAG and L to enhance the accessibility of the antibody

A

Gene	Nucleotide					Amino acid		
	Position	RefSeq	RNA-seq	Coverage	*p*-value	Position	RefSeq	RNA-seq
P	456	G	G 70.1%	144	8.4E-52	152	Met	Met
			A 29.9%					Ile
L	2762	U	G 100.0%	59		921	Leu	Arg
L	3334	U	G 100.0%	45		1112	Cys	Gly
L	3743	U	U 50.7%	64	1.2E-42	1248	Ile	Ile
			C 49.3%					Thr
L	4250	A	A 46.0%	84	5.9E-51	1417	Lys	Lys
			G 54.0%					Arg
L	4347	G	G 64.1%	85	4.9E-38	1449	Gly	Gly
			A 34.9%					Gly

B

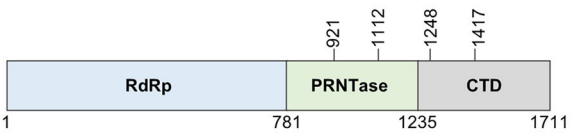

C

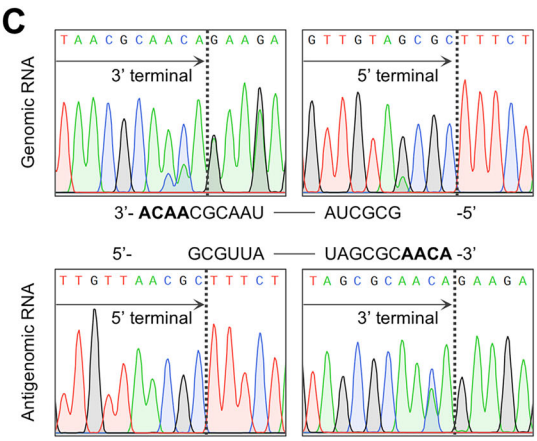

D

Sequence	3' terminal	5' terminal
RefSeq	3'- ACAACGCAAUUGUUG	CAACAUCGCGU -5'
RACE	3'- ACAACGCAAUUGUUG	CAACAUCGCG -5'

Fig. 1 | Reassessment of the complete genome sequence of BoDV-2. A Sequence analysis of total RNA extracted from BoDV-2 isolate No/98-infected Vero cells. Compared to the reference sequence (RefSeq) of BoDV-2 (accession no. AJ311524), substituted nucleotides in the reassessed sequence are represented in bold orange, and their percentages of the total are indicated. Concomitant amino acid changes are also represented in bold orange. **B** Schematic representation of BoDV-2 L. The putative RNA-dependent RNA polymerase (RdRp) domain, polyribonucleotidyltransferase (PRNTase) domain, and C-terminal domain (CTD) are colored blue, green, and gray, respectively. **C** RACE analysis of the 5' and 3' terminal sequences of both the genome and antigenome of BoDV-2. The 5' and 3' ends of total RNA extracted from BoDV-2-infected Vero cells were ligated with each oligoRNA. BoDV-2-specific 5' and 3' terminal sequences were amplified via RT-PCR and analyzed via direct sequencing. The border between the viral terminal sequence and ligated oligoRNA is indicated by the dotted line. The analyzed terminal sequences are indicated schematically. **D** Comparison of the reassessed genomic terminal sequences of BoDV-2 with the reference sequence.

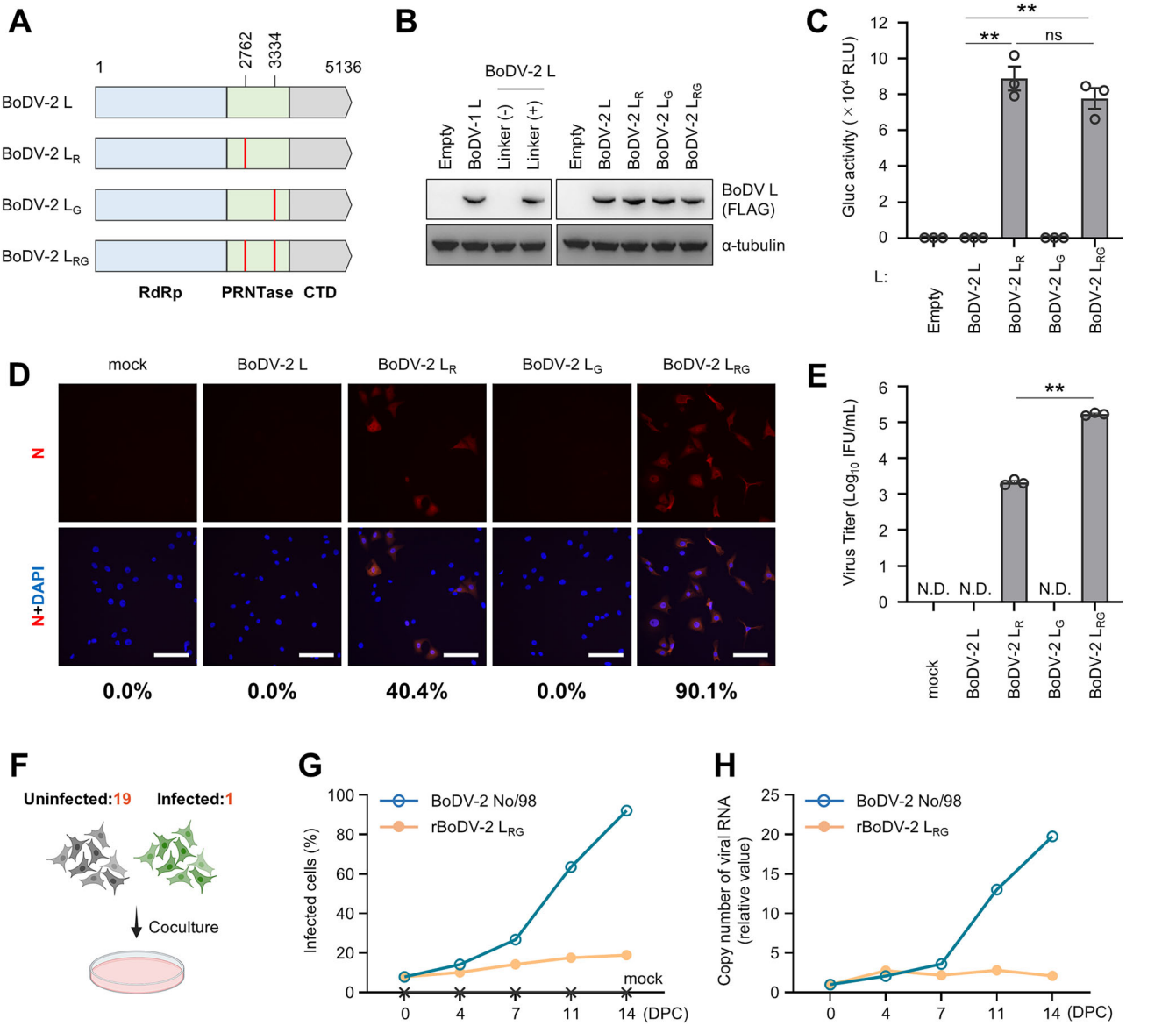

Fig. 2 | The polymerase activity of BoDV-2 L is restored by substituting a nucleotide. A Schematic representation of the BoDV-2 L gene variants inserted into the expression plasmid and the full-length BoDV-2 cDNA plasmid. The positions of the substituted nucleotides compared to the reference sequence are indicated by red bars. The putative RdRp domain, PRNTase domain, and CTD are colored blue, green, and gray, respectively. **B** Detection of BoDV-2 L variants by western blotting analysis. Whole-cell lysates were prepared from 293T cells transfected with the indicated plasmid. The primary antibodies used for detection are indicated to the right of the panels. Alpha-tubulin was used as the loading control. The original scans of these blots are shown as supplementary Figure 1. **C** BoDV-2 minireplicon assay using the indicated BoDV-2 L variants and BoDV-2 N and P as helper plasmids. Data are presented as the means ± standard errors of the means (± SEM) of three biologically independent experiments. One-way analysis of variance (ANOVA) and Tukey's multiple comparisons test were performed for statistical analysis. ns, not significant; $^{**}p < 0.01$; Gluc, *Gaussia* luciferase; RLU, relative light unit. **D**, **E** Rescue of rBoDV-2 by reverse genetics. Reverse genetics was performed by transfecting a BoDV-2 cDNA plasmid possessing the indicated substitution in the L gene and five helper plasmids into HEK293T cells. At 3 days post transfection, transfected HEK293T cells were cocultured with uninfected Vero cells. **D** After 14 days of cocultur, Vero cells were subjected to immunofluorescence assay (IFA) and the infected ratio was measured. Nuclei were counterstained with DAPI. Bar, 50 µm. **E** After 14 days of coculture, rBoDV-2 was prepared from cocultured Vero cells and inoculated into uninfected Vero cells. Cells were subjected to IFA at 72 h post inoculation and virus titer was calculated. (F to H) Growth kinetics assay of rBoDV-2. **F** Schematic representation of the growth kinetics assay. Vero cells infected with BoDV-2 isolate No/98 or with rBoDV-2 L_{RG} were cocultured with uninfected Vero cells at a ratio of 1 to 19 and passaged every 3 or 4 days. **G** The percentage of infected cells was determined by IFA using an antibody against BoDV N. DPC, days post coculture. **H** The copy number of viral RNA was measured via RT-qPCR using the total RNA extracted from each cells. DPC, days post coculture.

to the tag (Fig. 2B). In addition, we confirmed comparable expressions of the reconstructed BoDV-2 L variants in transfected cells in both mRNA (supplementary Fig. 2) and protein levels (Fig. 2B).

To determine the polymerase activities of the reconstructed BoDV-2 L variants, we performed a BoDV-2 minireplicon assay. As shown in Fig. 2C, reporter activity was not detected for BoDV-2 L with the reference sequence, indicating that it lacks any polymerase activity. Interestingly, BoDV-2 L possessing a nucleotide substitution at position 2762, namely, BoDV-2 L_R, restored its polymerase activity, whereas a substitution at position 3334, namely, BoDV-2 L_G, did not (Fig. 2C). Accordingly, BoDV-2 L_{RG}, which possesses both nucleotide substitutions simultaneously, exhibited the same level of polymerase activity as BoDV-2 L_R (Fig. 2C), indicating that a difference in the nucleotide at position 2762 is detrimental to the polymerase activity of BoDV-2 L.

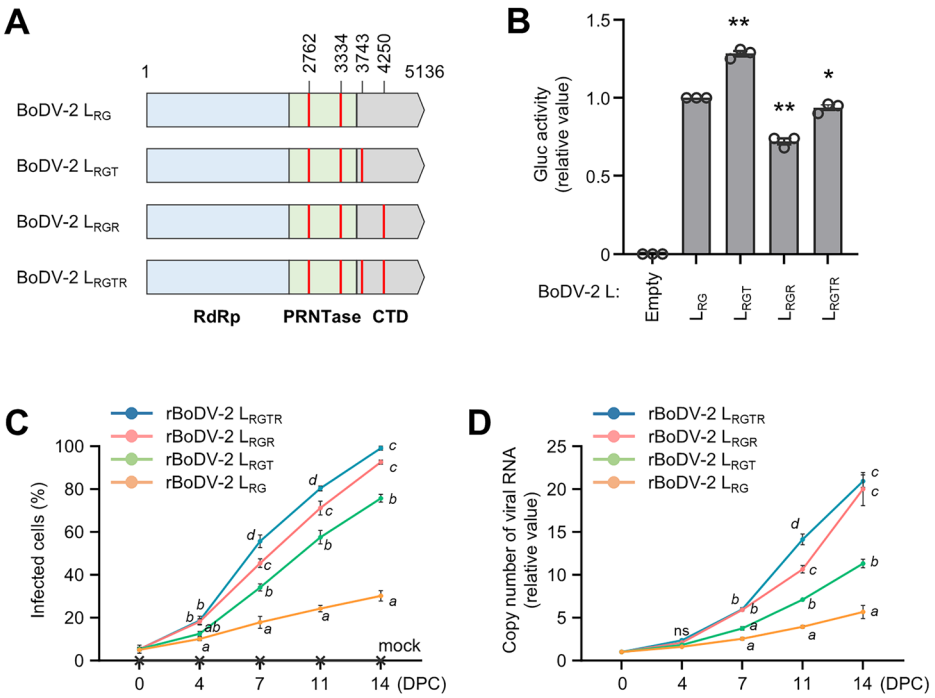

Fig. 3 | Nonsynonymous SNPs in the L gene facilitate the growth of BoDV-2. **A** Schematic representation of the BoDV-2 L gene variants inserted into the expression plasmid and the full-length BoDV-2 cDNA plasmid. The positions of the substituted nucleotides compared to the reference sequence are indicated by red bars. The putative RdRp domain, PRNTase domain, and CTD are colored blue, green, and gray, respectively. **B** BoDV-2 minireplicon assay using the indicated BoDV-2 L variants and BoDV-2 N and P as helper plasmids. Values for Gluc activity were normalized to that of the L_{RG} variant as a relative value of 1.0. Data are presented as the means ± SEM of three biologically independent experiments. One-way ANOVA and Dunnett's multiple comparisons test were performed for statistical analysis. $^{*}p < 0.05$; $^{**}p < 0.01$. **C**, **D** Growth kinetics assay of rBoDV-2 variants. Vero cells infected with the indicated rBoDV-2 were cocultured with uninfected Vero cells at a ratio of 1 to 19 and passaged every 3 or 4 days. DPC, days post coculture. **C** The percentage of infected cells was determined by IFA using an antibody against BoDV N. **D** The copy number of viral RNA was measured via RT-qPCR using total RNA extracted from each cells. Data are presented as the means ± SEM of three biologically independent experiments. Two-way ANOVA and Tukey's multiple comparisons test were performed for statistical analysis. Different characters (a, b, c) represent statistically significant differences at $p < 0.05$; ns, not significant.

To examine whether nucleotide differences at positions 2762 and 3334 of the L gene affect recovery of rBoDV-2 via reverse genetics, we constructed BoDV-2 cDNA plasmids expressing the full-length BoDV-2 antigenomes possessing each or both nucleotide substitutions. HEK293T cells were transfected with each BoDV-2 cDNA plasmid and five helper plasmids and cocultured with uninfected Vero cells at 3 days post transfection. After two weeks from coculture, rBoDV-2s that contain a nucleotide substitution at position 2762 of the L gene, rBoDV-2 L_R and L_{RG}, were successfully rescued (Fig. 2D and Supplementary Fig. 3). Interestingly, although nucleotide substitution at position 3334 did not affect the polymerase activity of BoDV-2 L in the minireplicon assay (Fig. 2C), rBoDV-2 L_{RG}, which possesses both substitutions at positions 2762 and 3334, seemed to be recovered more efficiently than rBoDV-2 L_R, which possesses a substitution at position 2762 alone (Fig. 2D). In addition, approximately 80-fold higher titer of rBoDV-2 L_{RG} was rescued compared with rBoDV-2 L_R (Fig. 2E), suggesting that the amino acid at position 1112 of the L also plays a role in BoDV-2 replication. To examine the growth ability of rBoDV-2 L_{RG} in comparison with that of the nonrecombinant BoDV-2 isolate No/98, Vero cells infected with rBoDV-2 L_{RG} or isolate No/98 were cocultured with uninfected Vero cells at a ratio of 1 to 19 (Fig. 2F), and viral propagation and the copy number of viral RNA were evaluated every 3 or 4 days by immunofluorescence assay (IFA) and RT-qPCR, respectively. While the nonrecombinant isolate No/98 spread to almost all Vero cells within 2 weeks of coculture, infection of rBoDV-2 L_{RG} exhibited limited spread within this period (Fig. 2G). Similarly, the copy number of viral RNA increased 20-fold in isolate No/98-infected cells, whereas it barely increased in rBoDV-2 L_{RG}-infected cells (Fig. 2H). These results suggest that the growth ability of rBoDV-2 is not only determined by the L2762 and L3334 substitutions, even though both substitutions induce high polymerase activity in the minireplicon assay.

Nonsynonymous SNPs in the L gene facilitate the growth of BoDV-2

Sequence analysis identified two nonsynonymous SNPs in the CTD of the L gene (Fig. 1A), indicating that the Vero cells persistently infected with BoDV-2 isolate No/98 contain a viral L quasispecies. Therefore, we constructed L expression plasmids harboring each or both nucleotide substitutions at positions 3743 and 4250 based on BoDV-2 L_{RG} and performed a minireplicon assay (Fig. 3A). While the substitution of uracil at position 3743 with cytosine, L_{RGT}, increased polymerase activity by 1.3-fold, that of adenine at position 4250 with guanine, L_{RGR}, decreased it by 0.7-fold. Substitution of both nucleotides, L_{RGTR}, slightly decreased polymerase activity (Fig. 3B).

To further investigate the impact of these SNPs on the growth ability of BoDV-2, we generated rBoDV-2 possessing each or both substitutions in the L gene and evaluated their growth kinetics. Although the substitution at position 4250 of the L gene had a detrimental effect on polymerase activity in the minireplicon assay (Fig. 3B), L proteins possessing either SNP substitution remarkably facilitated viral propagation and RNA synthesis of rBoDV-2 (Fig. 3C and D). These findings suggest that these SNPs influence viral replication through mechanisms other than enhancing polymerase activity in cells.

A nonsynonymous SNP in the P gene expedites the growth of BoDV-2

We also identified another nonsynonymous SNP at position 456 of the P gene (Fig. 1A). The P gene encodes the viral polymerase cofactor, which directly interacts with the L protein and plays a crucial role in viral polymerase activity[24,25]. Therefore, we examined the effects of this SNP on viral polymerase activity and viral growth ability using both a minireplicon

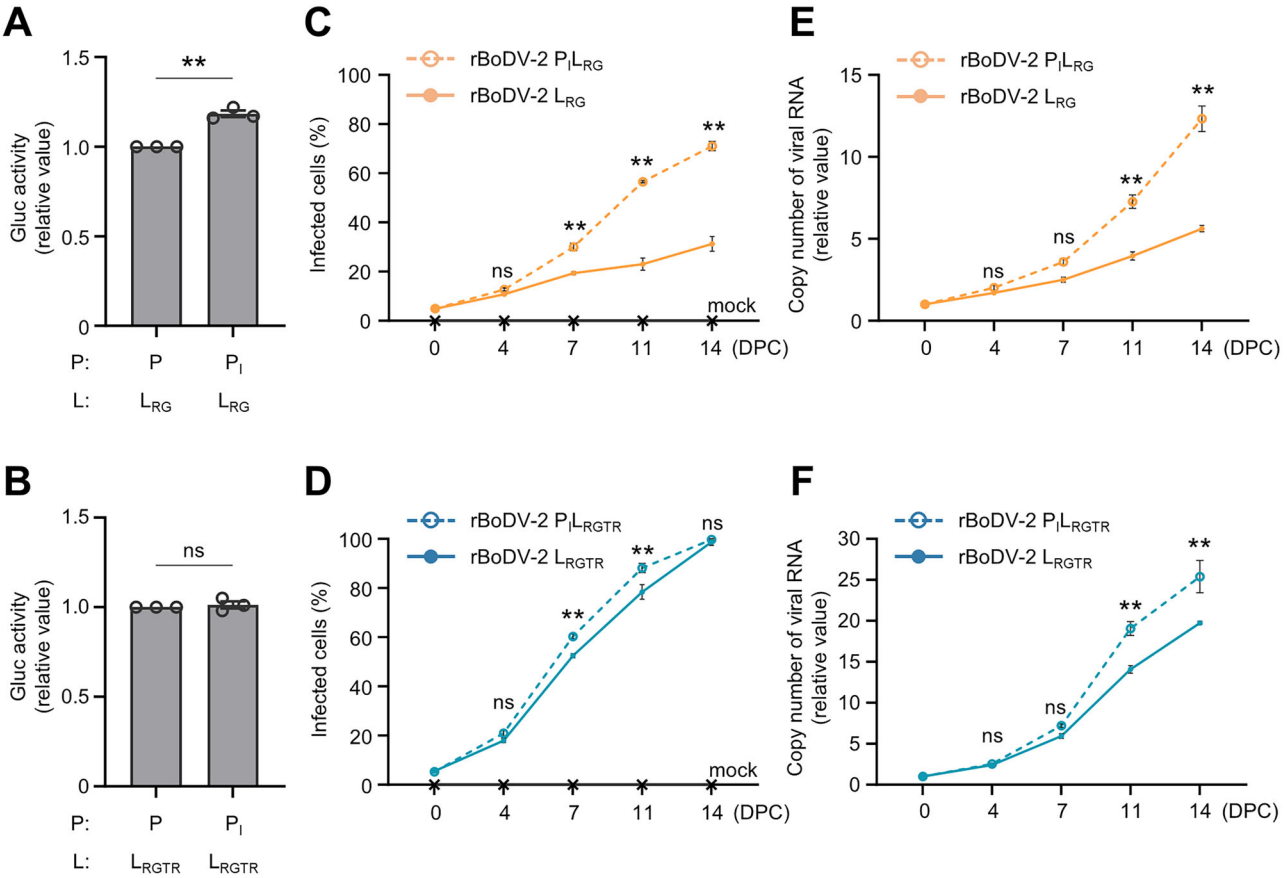

Fig. 4 | A nonsynonymous SNP in the P gene expedites the growth of BoDV-2. **A**, **B** BoDV-2 minireplicon assays using the indicated BoDV-2 P variants and BoDV-2 N and (A) L_{RG} or (B) L_{RGTR} as helper plasmids. Data are presented as the means ± SEM of three biologically independent experiments. An unpaired *t*-test was performed for statistical analysis. ns, not significant; $^{**}p < 0.01$. **C**–**F** Growth kinetics assay of rBoDV-2 variants. Vero cells infected with the indicated rBoDV-2 were cocultured with uninfected Vero cells at a ratio of 1 to 19 and passaged every 3 or 4 days. DPC, days post coculture. **C**, **D** The percentage of infected cells was determined by IFA using an antibody against BoDV N. **E**, **F** The copy number of viral RNA was measured via RT-qPCR using total RNA extracted from each cells. The data are presented as the means ± SEM of three biologically independent experiments. Two-way ANOVA and Tukey's or Sidak's multiple comparisons test were performed for statistical analysis. $^{**}p < 0.01$; ns, not significant.

assay and rBoDV-2 variants. Substitution of guanine at position 456 of the P gene with adenine, P_I, resulted in a slight increase in the polymerase activity of L_{RG} but not that of L_{RGTR}, as observed in the minireplicon assay (Fig. 4A and B). Furthermore, the P gene with the introduced SNP significantly facilitated viral propagation (Fig. 4C and D) and RNA synthesis of rBoDV-2 (Fig. 4E and F). These observations indicate that the nonsynonymous SNP detected in the P gene also contributed to the increase in rBoDV-2 growth ability.

Lack of superinfection exclusion maintains the low-fitness polymorphism in cells persistently infected with BoDV-2

Since the isolation of BoDV-2 isolate No/98 from a pony brain in 1999, it has been maintained for a long time in persistently infected Vero cells. Notably, although BoDV-2-infected Vero cells have undergone repeated passages, these SNPs, which significantly attenuate viral replication ability, were stably maintained within persistently infected cells (Fig. 1A). The coexistence of viral quasispecies in infected cells has been shown to affect overall viral replication and pathogenicity and therefore plays a role in the adaptation and evolution of viral populations[26].

To determine the significance of the coexistence of BoDV-2 quasispecies in infected cells, we performed infection experiments using cells infected with different sequences of rBoDV-2. First, we generated rBoDV-2 with different fluorescent marker genes, mCherry and GFP, inserted into the artificial intergenic region between the P and M genes (Fig. 5A) based on rBoDV-2 P_IL_{RGTR} with high-growth ability. As shown in Fig. 5B, both viruses exhibited similar growth kinetics, confirming that the effects of these two fluorescence marker proteins on the growth ability of BoDV-2 are not different. We therefore examined the propagation of rBoDV-2 variants with different growth abilities, namely, low-growth rBoDV-2 L_{RG}-mCherry (L_{RG}-mCherry) and high-growth rBoDV-2 P_IL_{RGTR}-GFP (P_IL_{RGTR}-GFP), by a competition assay using Vero cells infected with each recombinant virus. When Vero cells infected with L_{RG}-mCherry or P_IL_{RGTR}-GFP were cocultured with uninfected Vero cells at a ratio of 1:1:23, P_IL_{RGTR}-GFP rapidly spread throughout the culture, and the number of mCherry-expressing cells gradually decreased (Fig. 5C). Similarly, after 14 days of coculture, the genomic RNA of P_IL_{RGTR}-GFP accounted for almost all the BoDV-2 genomic RNA in the population (Fig. 5D and Supplementary Table. 1). These results suggest that if the viruses can spread into uninfected cells, a virus with high-growth ability spreads preferentially and occupies the majority of the population. However, we noticed that at 14 days after coculture, almost 1.0% of the cells coexpressed mCherry and GFP, and the proportion of cells expressing mCherry alone or coexpressing mCherry and GFP was approximately 3.3% of the total (Fig. 5C), indicating that high-growth P_IL_{RGTR}-GFP superinfected L_{RG}-mCherry-infected cells and that low-growth rBoDV-2 was maintained without elimination from the cells superinfected with the P_IL_{RGTR}-GFP. Therefore, to confirm the absence of superinfection exclusion between the rBoDV-2 variants, we next cocultured Vero cells infected with L_{RG}-mCherry and P_IL_{RGTR}-GFP at a 1:1 ratio. As a result, the percentage of cells coexpressing mCherry and GFP gradually increased; after 14 days of coculture, the proportions of cells expressing GFP

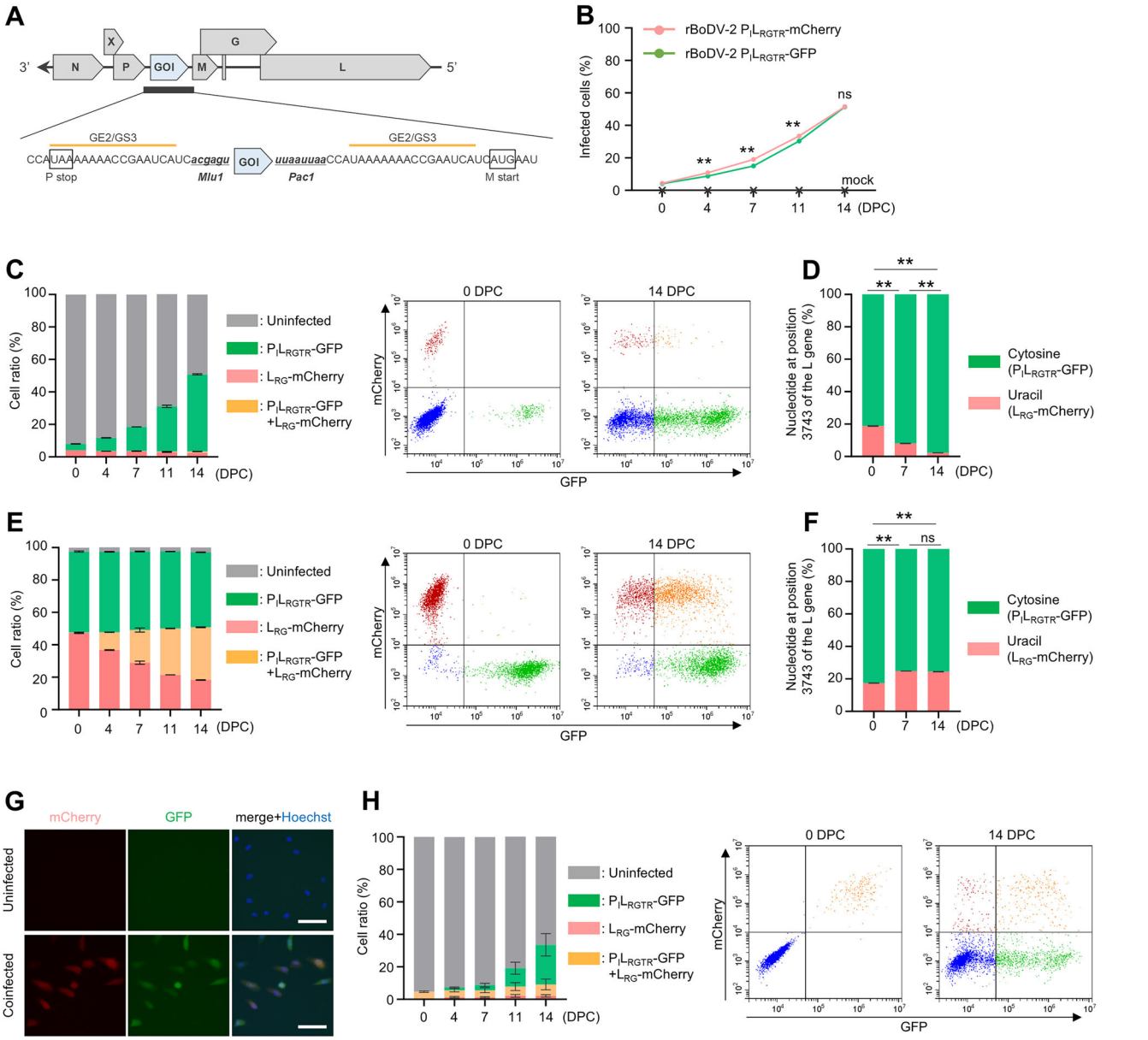

Fig. 5 | Lack of superinfection exclusion maintains the low-fitness polymorphism in cells persistently infected with BoDV-2. A Schematic representation of rBoDV-2 harboring an artificial expression cassette for the gene of interest (GOI) between the P and M genes. **B** Growth kinetics assay of rBoDV-2 harboring a fluorescent protein. Vero cells infected with rBoDV-2 P_IL_{RGTR}-mCherry or rBoDV-2 P_IL_{RGTR}-GFP were cocultured with uninfected Vero cells at a ratio of 1 to 19 and passaged every 3 or 4 days. The ratio of cells expressing fluorescent proteins was measured via flow cytometry. DPC, days post coculture. Data are presented as the means ± SEM of three biologically independent experiments. Two-way ANOVA and Sidak's multiple comparisons test were performed for statistical analysis. $^{**}p < 0.01$; ns, not significant. **C**, **D** Competition assay between rBoDV-2 L_{RG}-mCherry and rBoDV-2 P_IL_{RGTR}-GFP. The rBoDV-2 L_{RG}-mCherry-infected, rBoDV-2 P_IL_{RGTR}-GFP-infected, and uninfected Vero cells were cocultured at a ratio of 1 to 1 to 23 and passaged every 3 or 4 days. DPC, days post coculture. **C** The ratio of cells expressing fluorescent proteins was measured via flow cytometry. Representative data at 0 and 14 DPC are shown. **D** A nucleotide at position 3743 of the L gene was analyzed via amplicon sequencing, and the ratios of uracil to cytosine, which represent rBoDV-2 L_{RG}-mCherry and rBoDV-2 P_IL_{RGTR}-GFP, respectively, were compared. **E**, **F** Competition assay between rBoDV-2 L_{RG}-mCherry and rBoDV-2 P_IL_{RGTR}-GFP. The rBoDV-2 L_{RG}-mCherry-infected and rBoDV-2 P_IL_{RGTR}-GFP-infected Vero cells were cocultured at a ratio of 1 to 1 and passaged every 3 or 4 days. DPC, days post coculture. **E** The ratio of cells expressing fluorescent proteins was measured via flow cytometry. Representative data at 0 and 14 DPC are shown. **F** A nucleotide at position 3743 of the L gene was analyzed via amplicon sequencing, and the ratios of uracil to cytosine, which represent rBoDV-2 L_{RG}-mCherry and rBoDV-2 P_IL_{RGTR}-GFP, respectively, were compared. **G** Isolation of Vero cells coinfected with rBoDV-2 L_{RG}-mCherry and rBoDV-2 P_IL_{RGTR}-GFP. Bar, 50 μm. **H** Growth kinetics assay of rBoDV-2. Vero cells coinfected with rBoDV-2 L_{RG}-mCherry and rBoDV-2 P_IL_{RGTR}-GFP were cocultured with uninfected Vero cells at a ratio of 1 to 19 and passaged every 3 or 4 days. DPC, days post coculture. The ratio of cells expressing fluorescent proteins was measured via flow cytometry and representative data at 0 and 14 DPC are shown. **C**, **E**, and **H** Data are presented as the means ± SEM of three biologically independent experiments. **D**, **F** Data are presented as the means ± SEM of three biologically independent experiments. Two-way ANOVA and Sidak's multiple comparisons test were performed for statistical analysis. $^{**}p < 0.01$; ns, not significant.

alone, mCherry alone, and coexpressing mCherry and GFP were approximately 46.3%, 18.3%, and 32.4%, respectively (Fig. 5E). This finding suggests that the high-growth P_IL_{RGTR}-GFP predominantly superinfected to the L_{RG}-mCherry-infected cells. On the other hand, the proportion of viral genomic RNA of L_{RG}-mCherry in the culture increased to some extent (Fig. 5F and Supplementary Table. 2), indicating that the resident viruses were not eliminated even among the cells superinfected with the high-growth virus; rather, the replication of the low-growth viral genome was

upregulated by support from the polymerase derived from the high-growth virus in this experimental condition.

In addition, to investigate whether superinfection affects the propagation abilities of coinfected variants, we cloned Vero cells coinfected with both L_{RG}-mCherry and P_IL_{RGTR}-GFP (Fig. 5G) by the limiting dilution method and cocultured them with uninfected Vero cells at a ratio of 1 to 19. As shown in Fig. 5H, the proportion of cells infected with only the P_IL_{RGTR}-GFP virus increased; the L_{RG}-mCherry virus could also be transmitted to uninfected Vero cells, albeit only slightly. These observations suggest that BoDV-2 does not exclude superinfection, allowing low-fitness variants to persist within infected cells while maintaining their characteristics and thereby maintaining population diversity.

Discussion

In this study, to better understand the virological characteristics of BoDV-2, we reassessed the whole-genome sequence of BoDV-2 using RNA extracted from persistently BoDV-2-infected Vero cells. Compared to the original sequence of BoDV-2 isolate No/98, the reassessed sequence contains two nucleotide substitutions at positions 2762 and 3334 of the L gene, both of which induce an amino acid change in the PRNTase domain (Fig. 1A and B). Unfortunately, we cannot mention whether the reference sequence is correct because the exact propagation history of the isolate No/98-infected Vero is unknown, and we could not access the original stock. We found that the substitution of uracil at position 2762 with guanine alone is sufficient to restore the polymerase activity of BoDV-2 L and to recover rBoDV-2 by reverse genetics (Fig. 2). This nucleotide substitution induces an amino acid change from leucine to arginine at position 921 of L. Interestingly, arginine is completely conserved in the same position in all 47 sequences of BoDV-1 L registered in the database, suggesting that this positive-charged hydrophilic amino acid residue is critical for constructing the functional structure and polymerase activity of BoDV L. In contrast, the substitution of uracil at position 3334 with guanine, which induces an amino acid change from cysteine to glycine at position 1112 of L, did not affect the polymerase activity of BoDV-2 L in the minireplicon assay (Fig. 2C). However, interestingly, rBoDV-2 L_{RG}, which possesses amino acid substitutions at positions 921 and 1112, was rescued more efficiently than was rBoDV-2 L_R, which possesses a substitution at position 921 alone, by reverse genetics (Fig. 2D and E). This observation suggests that substitution at position 1112 may also play a critical role in the replication of BoDV-2 in a way other than enhancing polymerase activity, while position 1112 is located between the putative motif C (W) and motif D (HR) in the PRNTase domain, which is associated with the viral mRNA capping reaction[27]. In 47 sequences of BoDV-1 L registered on the database, alanine is completely conserved at position 1112, suggesting that an amino acid residue with a simple side chain is necessary at this position. Cysteine may not be suitable at this position because it can disrupt the structure and function of L by creating unrequested sulfate bindings. Further research such as structural analysis clarifies the mechanism of how the substitution at position 1112 plays a critical role in the replication of BoDV-2 in a way other than enhancing polymerase activity.

Our study showed that while rBoDV-2 could be rescued by substituting nucleotides at positions 2762 and 3334 of the L gene, the growth ability of rBoDV-2 L_{RG} was severely attenuated compared to that of the nonrecombinant BoDV-2 isolate No/98 (Fig. 2G and H). Interestingly, the substitution of nonsynonymous SNPs at positions 3743 and 4250 of the L gene significantly facilitated the growth ability of rBoDV-2 (Fig. 3C and D). Nucleotide substitution of uracil at position 3743 with cytosine induces an amino acid change from isoleucine to threonine at amino acid position 1248 of BoDV-2 L. Either isoleucine or threonine is conserved at the same position in BoDV-1 Ls in the database at a similar ratio, though it remains unclear whether substitution of isoleucine with threonine also affects the viral growth ability of BoDV-1. In addition, nucleotide substitution of alanine at position 4250 with guanine induces an amino acid change from lysine to arginine at amino acid position 1417 of BoDV-2 L. All the BoDV-1 Ls in the database except for that of strain CRNP5, which was generated by several passages of isolate He/80 in the brains of Lewis rats and SJL mice, show conservation of a lysine residue at the same amino acid position corresponding to 1417 of BoDV-2 L[28], but it is unclear whether rBoDV-1 possessing arginine residue at this position shows efficient propagation compared to the parental BoDV-1 isolate He/80[29]. Although both amino acids are located in CTD (Fig. 1B), no functional motifs or signal sequences have been reported in the CTD of BoDV L. In other mononegaviruses such as vesicular stomatitis virus, L interacts with P via multiple amino acid residues located in the CTD[30]. In addition, we previously identified 77 host proteins that interact with BoDV-1 L by using BioID2 assay, although the binding motifs have not been determined[31]. Therefore, these SNPs may affect the strength of the interaction of BoDV L with host and/or viral proteins, thereby enhancing the efficiency of viral replication through mechanisms other than enhancing polymerase activity. Investigating how these SNPs affect viral replication may help to elucidate the previously unknown role of the CTD of BoDV L.

In this study, we also identified one nucleotide substitution within an SNP at position 456 of the P gene. This substitution leads to an amino acid change from methionine to isoleucine at position 152, which facilitates the growth ability of rBoDV-2 (Fig. 4). BoDV-1 P interacts with P and L through binding domains spanning amino acid positions 135 to 172 and 135 to 183, respectively[25,32]. Additionally, previous research has indicated the presence of a nuclear export signal between amino acid positions 145 and 165 within BoDV-1 P[33]. Although the role of the amino acid residue in BoDV-1 P, corresponding to position 152 in BoDV-2 P, has yet to be explored, investigating its potential binding interactions with other viral proteins and its influence on the nuclear translocation capability of P would be of considerable interest.

Detection of 3 major nonsynonymous SNPs suggests that multiple distinct genotypes might exist within persistently infected Vero cells. BoDV-2 was initially isolated from the brain of an infected pony using primary young rabbit brain cells and subsequently propagated in Vero cells[5], after which the infected Vero cells were maintained for two decades. Due to the lack of original cell stocks and detailed passaging history, it is unclear when and how BoDV-2 acquired the P and L gene SNPs that we found in this study. However, given the comparable proportion of genome sequences containing SNPs, even those associated with low-fitness effects on propagation in culture, it may be possible that these SNPs were acquired after isolation in vitro to maintain persistent infection within cultured cells. On the other hand, our analysis revealed that BoDV-2 does not exhibit superinfection exclusion, even toward low-fitness mutant viruses (Fig. 5). From this observation, it is conceivable that viruses with different sequences may have coexisted before isolation. To better understand the characteristics and evolution of BoDV-2 infection, it is necessary to examine in detail the competition for growth between viruses with genomic variants not only in vitro but also in vivo.

In this study, we demonstrated that rBoDV-2 can infect cells infected with another rBoDV-2 with different replication abilities (Fig. 5C and E), showing that BoDV-2 does not exhibit superinfection exclusion. Superinfection exclusion is a common strategy used by many viruses to prevent sequential infection by closely related viruses[34,35]. For instance, substantial infection of influenza A virus (IAV) in cells that are already infected with IAV is inhibited by the active viral replication complex[36]. It has been reported that IAV superinfection exclusion constrains interactions between viral populations locally within a host to regulate viral fitness and evolution[37]. While superinfection exclusion provides evolutionary advantages for controlling viral fitness and population diversity, it also has the effect of promoting founder effects and reducing diversity and is thought to control the balance between genetic diversification and genome integrity in infected hosts[26]. A simulation study demonstrated that although a mutant with superinfection exclusion can overtake a population that cannot exclude superinfection, superinfection enables a population to adapt to environmental changes, indicating that superinfection exclusion negatively affects

the adaptation of a viral population in the long term[38]. These observations suggest that maintenance of genetic diversity through the absence of superinfection exclusion during BoDV-2 infection may play a pivotal role in the establishment of persistent infection. This might be achieved by not excluding low-fitness variants that may regulate replication dynamics and cytopathic effects as a viral population in infected cells. This hypothesis warrants a long-term in vivo infection experiment with several genotypes or strains of BoDVs.

In previous studies, BoDV-1 superinfection in cells persistently infected with BoDV-1 was demonstrated to be excluded both in vivo and in vitro[39,40]. The authors cocultured UTA6 human osteosarcoma cells persistently infected with the BoDV-1 isolate He/80 with either uninfected or BoDV-1 isolate H215-infected Vero cells and evaluated infection of isolate He/80 to Vero cells by IFA using a monoclonal antibody that reacts with the N of He/80 but not with the N of H215. Although infection of the isolate He/80 spread efficiently from the UTA6 cells to uninfected Vero cells, the infection did not spread to the H215-infected Vero cells after 3 weeks of coculture[40]. The authors further demonstrated that expression of either N, accessory protein (X), or P is sufficient to inhibit superinfection with BoDV-1, concluding that the imbalance in intracellular levels of vRNP components is attributable to superinfection exclusion of BoDV-1[40]. However, whereas the growth abilities of both the BoDV-1 isolates H215 and He/80 were high enough for the infection to spread efficiently in the previous study, the growth ability of the two different rBoDV-2s was significantly different in our experiments (Fig. 5C). In addition, the methods used to detect superinfection differed between these studies. Thus, further studies are necessary to investigate whether the absence of superinfection exclusion is a specific property for BoDV-2 but not for BoDV-1.

In conclusion, we successfully established a reverse genetics system for BoDV-2 and revealed lack of superinfection exclusion enables BoDV-2 to maintain the genetic diversity in persistently infected cells. Our study provides valuable insights into the biological properties of BoDV-2 and contributes to development of effective vaccines and antiviral drugs for pathogenic mammalian orthobornaviruses.

Materials and methods

Cell culture

Human embryonic kidney (HEK) 293 T cells were cultured in Dulbecco's modified Eagle's medium (DMEM) (Nacalai Tesque, Japan; #08456-36) supplemented with 10% fetal bovine serum (FBS) (Thermo Fisher Scientific, USA; #10270-106) and 1% penicillin-streptomycin-amphotericin B solution (Fujifilm, Japan; #161-23181). African green monkey kidney Vero cells were cultured in DMEM supplemented with 5% FBS and 1% penicillin-streptomycin-amphotericin B solution.

Virus

Vero cells persistently infected with BoDV-2 isolate No/98 were kindly provided by Prof. Martin Schwemmle (University of Freiburg, Germany) and propagated by Dennis Rubbenstroth's group at the Friedrich-Loeffler-Institut (FLI), Greifswald, Germany. Isolate No/98 had originally been isolated using primary young rabbit brain cells, which were subsequently cocultured with Vero cells. After consecutive passages, only Vero cells remained in the culture[5]. The exact propagation history of the isolate No/98-infected culture is unknown.

Sequencing of the viral genome

Total RNA was extracted from persistently BoDV-2-infected Vero cells using Agencourt® RNAdvance Tissue kit (Beckman Coulter) and the KingFisher Flex system (Thermo Fisher Scientific) according to manufacturers' instructions. Subsequently, cDNA synthesis and library preparation were performed as described in Wylezich et al.[41] and Calvelage et al.[42] with slight modifications. Briefly, cDNA was synthesized using the SuperScript IV First-Strand cDNA Synthesis System (Thermo Fisher Scientific) and subsequently, the complete reaction was used for 2nd strand synthesis with the NEBNext Ultra II Non-Directional RNA Second Strand Synthesis Module (New England Biolabs), followed by DNA fragmentation with a Covaris M220 and library preparation with a GeneRead DNA Library L Core kit (QIAGEN) and ION Xpress Barcode adapters (Thermo Fisher Scientific). After size selection, library size was measured using a 2100 BioAnalyzer system (Agilent Technologies) with Agilent High Sensitivity DNA Chip and reagents, and the library was quantified using a QIAseq Library Quant Assay Kit (Qiagen). The library was prepared for sequencing and sequenced together with Ion Torrent Calibration Standard (Thermo Fisher Scientific) using an Ion Torrent S5 XL instrument with Ion 530 chip and reagents (Thermo Fischer Scientific) in 400 bp mode.

We performed genome assembly as described in Calvelage et al.[43]. Sequencing adapters were trimmed using the Newbler assembler of the 454 Genome Sequencer Software Suite v. 3.0 (Roche) and the FastQC was used to quality control the sequence dataset. Initial reference-based mapping (454 Genome Sequencer Software Suite v. 3.0, Roche) against RefSeq BoDV-2 strain No/98 complete genome (AJ311524) was performed to generate a sample-specific consensus sequence. This consensus sequence was used as a reference for the second round of reference-based mapping analysis. Pairwise sequence alignment of the resulting BoDV-2 genome sequence and BoDV-2 AJ311524.1 was performed using MUSCLE[44]. This alignment was visually inspected with Geneious Prime® 2019.2.3 Software (Biomatters).

SNPs within the BoDV-2 genome were detected using the Find Variations/SNPs program implemented in the Geneious Prime® 2019.2.3 software as described in the study of Caldwell et al.[45]. In this analysis, we used the consequence sequence and BAM file generated from the 2nd round of mapping analyses as data input. We performed variant calling under the following conditions: minimum coverage of aligned sequences and the minimum variant frequency is set to 50× and 25%, respectively. The "Find Variations/SNPs" algorithm also calculates *P*-values representing the probability of sequencing errors. We excluded any variant exceeding 10^{-7}, as a lower *p*-value increases the probability that the observed variation in a given position represents a real variant. We also excluded observed variants with *p*-value 10^{-5} when exceeding 65% strand bias.

RACE analysis

Total RNA extracted from BoDV-2-infected Vero cells was ligated with either 5' adaptor oligoRNA (5'-CGACUGGAGCACGAGGACACUGA CAUGGACUGAAGGAGUAGAAA (Thermo Fisher Scientific, USA; #L150201)) or 3' adaptor oligoRNA (5'-GAAGAGAAGGUGGAAAU GGCGUUUUGG; the 5' and 3' ends were modified with a monophosphate and an amino-modifier, respectively) using T4 RNA Ligase 1 (New England Biolabs, USA; #M0204) according to the manufacturer's instructions. The adaptor-ligated RNA was reverse transcribed using SuperScript IV Reverse Transcriptase (Thermo Fisher Scientific, USA; #18090010) and amplified by PCR using Q5 Hot Start High-Fidelity 2x Master Mix (New England Biolabs, USA; #M0494) according to the manufacturer's instructions. The viral terminal sequences were analyzed via Sanger sequencing of the purified PCR amplicons. The primers used in the RACE analysis are listed in the Table 1.

Plasmid construction

The plasmid used to express BoDV-2 N, P, and L were described previously[23]. Nucleotide substitutions in the P or L gene were introduced by PCR mutagenesis. A FLAG-tag sequence was inserted with a GS-linker sequence (5'- GGGAGTTCCGGTGGTGGCGGGAGCGGAGGTGGAG GCTCCAGTGGT) into the 5' terminus of the L gene by PCR mutagenesis. A plasmid expressing each BoDV-2 M or G was constructed by inserting each gene into the EcoRI and XhoI restriction enzyme recognition sites of the eukaryotic expression plasmid pCAGGS[46]. For both plasmids, synonymous substitutions were introduced by PCR mutagenesis into the splicing donor and acceptor sites to increase protein expression levels[20,47]. An RNA polymerase II (Pol II)-driven BoDV-2 minigenome plasmid was constructed similarly to the BoDV-1 minireplicon plasmid described previously[23]. In brief, a *Gaussia* luciferase (Gluc) reporter gene flanked by the 3' and 5' untranslated regions of BoDV-2 in the negative-sense

Table 1 | Primers used in the 5' and 3' RACE analysis for BoDV-2

Target	RT primer	PCR primer	
		Forward	Reverse
5' end of genome	5'-GCCTTATTTAAGCCCGTTTACAGG	5'-CGACTGGAGCACGAGGACACTGA	5'-GATGGACTTGGTCATGATTCGAGG
3' end of genome	5'-CCAAAACGCCATTTCCACCTTCTCTTC	5'-CCAAAACGCCATTTCCACCTTCTCTTC	5'-GAGGATATCTCTAACTCGGTGAGC
5' end of antigenome	5'-CAGCTCCAGCCTTAATCTTGG	5'-CGACTGGAGCACGAGGACACTGA	5'-GAGGATATCTCTAACTCGGTGAGC
3' end of antigenome	5'-CCAAAACGCCATTTCCACCTTCTCTTC	5'-CCAAAACGCCATTTCCACCTTCTCTTC	5'-GATGGACTTGGTCATGATTCGAGG

orientation was inserted into the XhoI and NotI restriction enzyme recognition sites of pCAG-HRSV3[48], with a hammerhead ribozyme (HamRz) sequence at the 5' end and a hepatitis delta virus ribozyme (HdvRz) sequence at the 3' end. A BoDV-2 cDNA plasmid that expresses the full-length antigenomic RNA of BoDV-2 strain No/98 was constructed similarly to the corresponding BoDV-1 cDNA plasmid described previously[49]. In brief, an artificially synthesized full-length cDNA identical to the published reference sequence of BoDV-2 isolate No/98 was inserted into the XhoI and NotI restriction enzyme recognition sites of pCAG-HRSV3[48] with an HamRz sequence at the 5' end and an HdvRz sequence at the 3' end. A BoDV-2 cDNA plasmid that harbors an additional expression cassette between the P and M genes was constructed by inserting a gene of interest flanked by the MluI and PacI restriction enzyme recognition sequences with the repeated 2nd gene end (GE2) and the 3rd gene start (GS3) signal sequences by PCR mutagenesis (Fig. 5A)[49].

Western blotting

Cultured cells were lysed with 1x sample buffer (50 mM Tris-HCl, pH 6.8; 2% sodium dodecyl sulfate (SDS); 5% w/v sucrose; and 5% 2-mercaptoethanol) followed by boiling at 95 °C for 10 min. Cell lysates were subjected to SDS-PAGE using an ePAGEL (ATTO Corporation, Japan; #2331720), and proteins were subsequently transferred to Trans-Blot® Turbo™ Mini nitrocellulose membranes (Bio-Rad, USA; #1704156). The membranes were blocked with blocking buffer (TBS containing 0.1% Tween-20 with 5% w/v skim milk) and then incubated with the 1:2000 diluted anti-FLAG M2 antibody (Sigma-Aldrich, USA; #F1804) or the 1:10000 diluted anti-alpha-tubulin antibody (Sigma-Aldrich, USA; #T5168), followed by incubation with the 1:5000 diluted secondary antibody (horseradish peroxidase (HRP)-conjugated anti-mouse IgG (Jackson ImmunoResearch, USA; #715-035-150)). The protein bands were detected with Clarity Western ECL substrate reagents (Bio-Rad, USA; #170-5060), and chemiluminescence signals were visualized by Fusion Solo S (Vilber, France).

BoDV-2 minireplicon assay

HEK293T cells seeded into 48-well plates were transfected with 50 ng of BoDV-2 minigenome plasmid, 50 ng of pCAGGS-BoDV-2 N, 5 ng of pCAGGS-BoDV-2 P, 50 ng of pCAGGS-BoDV-2 L, and 5 ng of control plasmid expressing *Cypridina* luciferase using TransIT293 (Mirus, USA; #MIR2700) according to the manufacturer's instructions. At 48 h post transfection, *Gaussia* luciferase and *Cypridina* luciferase expression levels were measured with a Biolux *Gaussia* luciferase assay kit (New England Biolabs, USA; #E3300) and Biolux *Cypridina* luciferase assay kit (New England Biolabs, USA; #E3309), respectively, according to the manufacturer's instructions. Luminescence signals were detected by a GloMax Discover Microplate Reader (Promega, USA), and polymerase activity was quantified by normalizing *Gaussia* luciferase activity to *Cypridina* luciferase activity.

Reverse genetics of BoDV-2

Reverse genetics was performed according to the protocol summarized in our previous review article[21]. HEK293T cells seeded into 6-well plates were transfected with 2.0 μg of BoDV-2 cDNA plasmid, 0.5 μg of pCAGGS-BoDV-2 N, 0.025 μg of pCAGGS-BoDV-2 P, 0.25 μg of pCAGGS-BoDV-1 L, 0.04 μg of pCAGGS-BoDV-2 M, and 0.01 μg of pCAGGS-BoDV-2 G using TransIT293 according to the manufacturer's instructions. At 3 days post transfection, the transfected cells were cocultured with uninfected Vero cells, which were passaged every 3 or 4 days until the infection spread to almost all the Vero cells. The transfected HEK293T cells were removed by adding 1.0 μg/mL puromycin (InvivoGen, USA; #ant-pr) to the culture medium at the optimal time point. For viral preparation, cocultured Vero cells were trypsinized, centrifuged, and resuspended in DMEM (Nacalai Tesque). Then, the cells were sonicated using Bioruptor® II (Sonicbio Co., Ltd., Japan) and centrifuged at 1200 × *g* for 25 min at 4 °C. The supernatant containing rBoDV-2 was used as a viral solution.

Immunofluorescence assay

Cultured cells were fixed with 4% paraformaldehyde (Nacalai Tesque, Japan; #09154-85) for 10 min and permeabilized with PBS containing 0.5% Triton X-100 (Wako, Japan; #169-21105) and 5% bovine serum albumin (Sigma-Aldrich, USA; #A3059) for 10 min. The cells were incubated with the 1:10,000 diluted anti-BoDV N antibody (HB01), followed by incubation with the 1:1,000 diluted Alexa Fluor® 555-conjugated anti-rabbit IgG antibody (Thermo Fisher Scientific, USA; #A21429) and 300 nM 4′,6′-diamidino-2-phenylindole (DAPI) (Merck, Germany; #28718-90-3). Fluorescence signals were observed by an ECLIPSE TE2000-U fluorescence microscope (Nikon, Japan).

RT-qPCR

Total RNA was extracted from cultured cells using NucleoSpin RNA Plus (Macherey-Nagle, Germany; #740984) according to the manufacturer's instructions. For detection of BoDV-2 RNA, RT-qPCR was performed using qScript XLT one-step RT-qPCR ToughMix Kit (Quanta Biosciences, USA; #95132) with forward primer (5'-TAGTYAGGAGGCT-CAATGGCA), reverse primer (5'-GTCCYTCAGGAGCTGGTC), and probe (5'-FAM-AAGAAGATCCCCAGACACTACGACG-BHQ1). Each reaction contained 2.75 μl of RNase-free water, 6.25 μl of 2x qScript XLT One-Step RT-qPCR ToughMix, 1.0 μl of primer-probe mix (7.5 pmol/μl primer and 2.5 pmol/μl probe) and 2.5 μl of RNA template (approximately 500 ng of total RNA) or RNase-free water for the no template control in a total volume of 12.5 μl. The thermal program consisted of 1 cycle of 50 °C for 10 min and 95 °C for 1 min, followed by 40 cycles of 95 °C for 10 s, 57 °C for 30 s, and 68 °C for 30 s[8]. For detection of GAPDH mRNA, approximately 500 ng of total RNA was reverse transcribed using the Verso cDNA synthesis kit (Thermo Fisher Scientific, USA; #AB1453) with anchored oligo dT primer according to the manufacturer's instructions. qPCR was performed using Luna Universal qPCR Master Mix (New England Biolabs, USA; #M3003) with forward (5'-ATCTTCTTTTGCGTCGCCAG) and reverse (5'-ACGACCAAATCCGTTGACTCC) primers. Each reaction contained 8.0 μl of RNase-free water, 10.0 μl of Luna Universal qPCR Master Mix, 1.0 μl of primer mixture (10.0 pmol/μl primer) and 1.0 μl of synthesized cDNA or RNase-free water for the no template control in a total volume of 20.0 μl. The thermal program consisted of 1 cycle of 95 °C for 1 min and 40 cycles of 95 °C for 10 s and 60 °C for 30 s, followed by a melting reaction. All reactions were performed with a CFX Connect real-time system (Bio-Rad, USA), and relative expression levels of BoDV-2 RNA were calculated via the relative quantification method with GAPDH mRNA serving as a reference.

Flow cytometry

Cultured cells were fixed with 4% paraformaldehyde for 20 min and suspended in PBS containing 2.0% FBS. Proportions of cells expressing either or both mCherry and GFP were analyzed by a CytoFLEX S flow cytometer (Beckman Coulter, USA). The criterion for assessing the extent of positive detection of each mCherry or GFP signal was set using mock-infected cells as a negative control.

Amplicon sequencing

Total RNA was extracted from cultured cells using NucleoSpin RNA Plus according to the manufacturer's instructions. BoDV-2 genomic RNA was reverse transcribed using SuperScript IV Reverse Transcriptase with a genome-specific primer (5'- AGGGACACTCTCGTTCTCCA) according to the manufacturer's instructions. To prepare the sequencing library, the 1st PCR product ranging from position 3556 to 3954 of the L gene was amplified from 1.0 µl of cDNA using Q5 Hot Start High-Fidelity 2x Master Mix with forward (5'-acactctttccctacacgacgctcttccgatctGGATGCCTCTAT GCTGACTCTG) and reverse (5'-gtgactggagttcagacgtgtgctcttccgatctACC AACCAGGAATCGCCAAA) primers. Then, amplicon sequencing was performed by the Bioengineering Lab. Co., Ltd. (Kanagawa, Japan). Briefly, the 2nd PCR product was amplified from 10 ng purified 1st PCR product using the TaKaRa Ex Taq HS (TaKaRa Bio Inc., Japan; #RR006A) with a forward (5'- AATGATACGGCGACCACCGAGATCTACAC-*Index2*-ACACTCTTTCCCTACACGACGC) and reverse (5'- CAAGCAGAA-GACGGCATACGAGAT-*Index1*-GTGACTGGAGTTCAGACGTGTG) primers. Sequencing of the purified 2nd PCR products was performed using the MiSeq system and MiSeq Reagent Kit v3 (Illumina, USA) with a 2 × 300 bp read length protocol. From the raw sequence reads, adaptor and primer sequences were removed using the FASTX Toolkit (ver. 0.0.14)[50]. Low-quality and short reads were also removed using Sickle (ver. 1.33) with criteria of a quality score of <Q20 and a read length of ≤40 bp[51]. Filtered high-quality reads were merged using FLASH (ver. 1.2.11) with default settings[52]. The number of each read was counted by a proprietary algorithm developed by the Bioengineering Lab. Co., Ltd. and summarized in an Excel file. Based on the Excel file, the ratio of U to C of the nucleotide at position 3743, representing rBoDV-2 L_{RG}-mCherry and P_IL_{RGTR}-GFP, respectively, was analyzed to distinguish two genotypes of rBoDV-2.

Statistical analysis

All statistical analyses were performed with GraphPad Prism 10 software. The tests used for each experiment are described in figure legends.

Data availability

The sequencing data of total RNA extracted from BoDV-2-infected Vero cells is deposited in the European Nucleotide Archive (ENA) under Sequence Read Archive accession number ERR14722785. Other data used and/or analyzed during the current study is demonstrated in this paper. Additional information is available from the corresponding author upon request.

Code availability

No custom code and scripts were used during data analysis. The versions of the software are described in Materials and Methods.

Received: 7 June 2024; Accepted: 4 April 2025;
Published online: 17 April 2025

References

1. Richt, J. A. & Rott, R. Borna disease virus: a mystery as an emerging zoonotic pathogen. *Vet. J.* **161**, 24–40 (2001).
2. Kinnunen, P. M., Palva, A., Vaheri, A. & Vapalahti, O. Epidemiology and host spectrum of Borna disease virus infections. *J. Gen. Virol.* **94**, 247–262 (2013).
3. Rubbenstroth, D. Avian Bornavirus Research-A Comprehensive Review. *Viruses* **14**, 1513 (2022).
4. Kuhn, J. H. et al. Annual (2023) taxonomic update of RNA-directed RNA polymerase-encoding negative-sense RNA viruses (realm Riboviria: kingdom Orthornavirae: phylum Negarnaviricota). *J. Gen. Virol*. **104**, 001864 (2023).
5. Nowotny, N. et al. Isolation and characterization of a new subtype of Borna disease virus. *J. Virol.* **74**, 5655–5658 (2000).
6. Pleschka, S. et al. Conservation of coding potential and terminal sequences in four different isolates of Borna disease virus. *J. Gen. Virol.* **82**, 2681–2690 (2001).
7. Korn, K. et al. Fatal Encephalitis Associated with Borna Disease Virus 1. *N. Engl. J. Med.* **379**, 1375–1377 (2018).
8. Schlottau, K. et al. Fatal Encephalitic Borna Disease Virus 1 in Solid-Organ Transplant Recipients. *N. Engl. J. Med.* **379**, 1377–1379 (2018).
9. Coras, R., Korn, K., Kuerten, S., Huttner, H. B. & Ensser, A. Severe bornavirus-encephalitis presenting as Guillain-Barre-syndrome. *Acta Neuropathol.* **137**, 1017–1019 (2019).
10. Liesche, F. et al. The neuropathology of fatal encephalomyelitis in human Borna virus infection. *Acta Neuropathol.* **138**, 653–665 (2019).
11. Niller, H. H. et al. Zoonotic spillover infections with Borna disease virus 1 leading to fatal human encephalitis, 1999–2019: an epidemiological investigation. *Lancet Infectious Dis.***20**, 467–477 (2020).
12. Eisermann, P. et al. Active Case Finding of Current Bornavirus Infections in Human Encephalitis Cases of Unknown Etiology, Germany, 2018-2020. *Emerg. Infect. Dis.* **27**, 1371–1379 (2021).
13. Tappe, D. et al. Investigation of fatal human Borna disease virus 1 encephalitis outside the previously known area for human cases, Brandenburg, Germany - a case report. *BMC Infect. Dis.* **21**, 787 (2021).
14. Frank, C. et al. Human Borna disease virus 1 (BoDV-1) encephalitis cases in the north and east of Germany. *Emerg Microbes Infect.* **11**, 6–13 (2022).
15. Grosse, L. et al. First detected geographical cluster of BoDV-1 encephalitis from same small village in two children: therapeutic considerations and epidemiological implications. *Infection*, 1–16 (2023).
16. Hoffmann, B. et al. A Variegated Squirrel Bornavirus Associated with Fatal Human Encephalitis. *N. Engl. J. Med.* **373**, 154–162 (2015).
17. Rubbenstroth, D., Schlottau, K., Schwemmle, M., Rissland, J. & Beer, M. Human bornavirus research: Back on track!. *PLoS Pathog.* **15**, e1007873 (2019).
18. Schneider, U., Schwemmle, M. & Staeheli, P. Genome trimming: a unique strategy for replication control employed by Borna disease virus. *Proc. Natl. Acad. Sci. USA.* **102**, 3441–3446 (2005).
19. Martin, A., Staeheli, P. & Schneider, U. RNA polymerase II-controlled expression of antigenomic RNA enhances the rescue efficacies of two different members of the Mononegavirales independently of the site of viral genome replication. *J. Virol.* **80**, 5708–5715 (2006).
20. Kanda, T., Sakai, M., Makino, A. & Tomonaga, K. Exogenous expression of both matrix protein and glycoprotein facilitates infectious viral particle production of Borna disease virus 1. *J. Gen. Virol*. **103** https://doi.org/10.1099/jgv.0.001767 (2022).
21. Kanda, T. & Tomonaga, K. Reverse Genetics and Artificial Replication Systems of Borna Disease Virus 1. *Viruses* **14**, 2236 (2022).
22. Martin, A., Hoefs, N., Tadewaldt, J., Staeheli, P. & Schneider, U. Genomic RNAs of Borna disease virus are elongated on internal template motifs after realignment of the 3' termini. *Proc. Natl. Acad. Sci. USA.* **108**, 7206–7211 (2011).
23. Kanda, T., Horie, M., Komatsu, Y. & Tomonaga, K. The Borna Disease Virus 2 (BoDV-2) Nucleoprotein Is a Conspecific Protein That Enhances BoDV-1 RNA-Dependent RNA Polymerase Activity. *J. Virol.* **95**, e0093621 (2021).
24. Walker, M. P., Jordan, I., Briese, T., Fischer, N. & Lipkin, W. I. Expression and characterization of the Borna disease virus polymerase. *J. Virol.* **74**, 4425–4428 (2000).

25. Schneider, U., Blechschmidt, K., Schwemmle, M. & Staeheli, P. Overlap of interaction domains indicates a central role of the P protein in assembly and regulation of the Borna disease virus polymerase complex. *J. Biol. Chem.* **279**, 55290–55296 (2004).
26. Andino, R. & Domingo, E. Viral quasispecies. *Virology* **479-480**, 46–51 (2015).
27. Ogino, T. & Banerjee, A. K. An unconventional pathway of mRNA cap formation by vesiculoviruses. *Virus Res.* **162**, 100–109 (2011).
28. Nishino, Y., Kobasa, D., Rubin, S. A., Pletnikov, M. V. & Carbone, K. M. Enhanced neurovirulence of borna disease virus variants associated with nucleotide changes in the glycoprotein and L polymerase genes. *J. Virol.* **76**, 8650–8658 (2002).
29. Ackermann, A., Kugel, D., Schneider, U. & Staeheli, P. Enhanced polymerase activity confers replication competence of Borna disease virus in mice. *J. Gen. Virol.* **88**, 3130–3132 (2007).
30. Liang et al. Structure of the L Protein of Vesicular Stomatitis Virus from Electron Cryomicroscopy. *Cell* **16**, 314–327 (2015).
31. Garcia, B. C. B., Horie, M., Kojima, S., Makino, A. & Tomonaga, K. BUD23-TRMT112 interacts with the L protein of Borna disease virus and mediates the chromosomal tethering of viral ribonucleoproteins. *Microbiol. Immunol.***65**, 492–504 (2021).
32. Schwemmle, M. et al. Interactions of the borna disease virus P, N, and X proteins and their functional implications. *J. Biol. Chem.* **273**, 9007–9012 (1998).
33. Yanai, H. et al. A methionine-rich domain mediates CRM1-dependent nuclear export activity of Borna disease virus phosphoprotein. *J. Virol.* **80**, 1121–1129 (2006).
34. Kumar, N., Sharma, S., Barua, S., Tripathi, B. N. & Rouse, B. T. Virological and Immunological Outcomes of Coinfections. *Clin. Microbiol. Rev*. **31**, e00111–17 (2018).
35. Laureti, M., Paradkar, P. N., Fazakerley, J. K. & Rodriguez-Andres, J. Superinfection Exclusion in Mosquitoes and Its Potential as an Arbovirus Control Strategy. *Viruses* **12**, 1259 (2020).
36. Sun, J. & Brooke, C. B. Influenza A Virus Superinfection Potential Is Regulated by Viral Genomic Heterogeneity. *mBio* **9**, e01761–18 (2018).
37. Sims, A. et al. Superinfection exclusion creates spatially distinct influenza virus populations. *PLoS Biol.* **21**, e3001941 (2023).
38. Hunter, M. & Fusco, D. Superinfection exclusion: A viral strategy with short-term benefits and long-term drawbacks. *PLoS Comput. Biol.* **18**, e1010125 (2022).
39. Formella, S., Jehle, C., Sauder, C., Staeheli, P. & Schwemmle, M. Sequence variability of Borna disease virus: resistance to superinfection may contribute to high genome stability in persistently infected cells. *J. Virol.* **74**, 7878–7883 (2000).
40. Geib, T. et al. Selective virus resistance conferred by expression of Borna disease virus nucleocapsid components. *J. Virol.* **77**, 4283–4290 (2003).
41. Wylezich, C., Papa, A., Beer, M. & Höper, D. A. Versatile Sample Processing Workflow for Metagenomic Pathogen Detection. *Sci. Rep.* **8**, 13108 (2018).
42. Calvelage, S. et al. Population- and Variant-Based Genome Analyses of Viruses from Vaccine-Derived Rabies Cases Demonstrate Product Specific Clusters and Unique Patterns. *Viruses* **12**, 115 (2020).
43. Calvelage, S. et al. Full-Genome Sequences and Phylogenetic Analysis of Archived Danish European Bat Lyssavirus 1 (EBLV-1) Emphasize a Higher Genetic Resolution and Spatial Segregation for Sublineage 1a. *Viruses* **13**, 634 (2021).
44. Edgar, R. C. MUSCLE: multiple sequence alignment with high accuracy and high throughput. *Nucleic Acids Res.* **32**, 1792–1797 (2004).
45. Caldwell, H. S., Lasek-Nesselquist, E., Follano, P., Kramer, L. D. & Ciota, A. T. Divergent Mutational Landscapes of Consensus and Minority Genotypes of West Nile Virus Demonstrate Host and Gene-Specific Evolutionary Pressures. *Genes* **11**, 1299 (2020).
46. Niwa, H., Yamamura, K. & Miyazaki, J. Efficient selection for high-expression transfectants with a novel eukaryotic vector. *Gene* **108**, 193–199 (1991).
47. Sakai, M. et al. Optimal expression of the envelope glycoprotein of orthobornaviruses determines the production of mature virus particles. *J. Virol*. **95**, e02221–20 (2020).
48. Yanai, H. et al. Development of a novel Borna disease virus reverse genetics system using RNA polymerase II promoter and SV40 nuclear import signal. *Microbes Infect.* **8**, 1522–1529 (2006).
49. Daito, T. et al. A novel borna disease virus vector system that stably expresses foreign proteins from an intercistronic noncoding region. *J. Virol.* **85**, 12170–12178 (2011).
50. Gordon, A. & Hannon, G. J. Fastx-toolkit. FASTQ/A short-reads pre-processing tools. *FASTQ/A short-reads preprocessing tools (unpublished)* **5**, https://github.com/agordon/fastx_toolkit (2010).
51. Joshi, N. & Fass, J. Sickle: a sliding-window, adaptive, quality-based trimming tool for FastQ files (version 1.33). https://github.com/najoshi/sickle (2011).
52. Magoč, T. & Salzberg, S. L. FLASH: fast length adjustment of short reads to improve genome assemblies. *Bioinformatics* **27**, 2957–2963 (2011).

Acknowledgements

We are grateful to Prof. Martin Schwemmle (University of Freiburg, Germany) for providing BoDV-2-infected Vero cells and to Andrea Aebischer, Sten Calvelage, Doreen Schulz, Patrick Zitzow, and Kathrin Steffen (Friedrich-Loeffler-Institute, Germany) for their technical support. We also thank Prof. Masayuki Horie (Osaka Metropolitan University, Japan) for supporting bilateral research.This study was supported in part by JSPS KAKENHI grants JP19J23468 (T.K.), JP22K20507 (T.K.), JP23K14083 (T.K.), JP19K22530 (K.T.), JP20H05682 (K.T.), and JP21K19909 (KT); JSPS Overseas Challenge Program for Young Researchers grant 202080194 (T.K.); JSPS Core-to-Core Program JPJSCCA20190008 (K.T.); Kaketsuken Research Grant (K.T.); the Joint Usage/Research Center Program on Institute for Life and Medical Sciences, Kyoto University (K.T.); Institute for Life and Medical Sciences Office of Directors' Research Grants Program, Kyoto University (T.K.); and the German Federal Ministry of Education and Research, Zoonotic Bornavirus Consortium (ZooBoCo), grants 01KI1722 and 01KI2005 (D.R., M.B., and D.H.).

Author contributions

T.K. and D.R. designed the study. T.K., P.D.S., D.H., and D.R. performed experiments and analyzed data. M.B., D.R., and K.T. supervised the project. T.K. and K.T. wrote the manuscript.All authors reviewed and approved the manuscript.

Competing interests

The authors declare no competing interests.

Additional information

Supplementary information The online version contains supplementary material available at https://doi.org/10.1038/s44298-025-00117-w.

Correspondence and requests for materials should be addressed to Dennis Rubbenstroth or Keizo Tomonaga.